Electronic Supplementary Material (ESI) for Dalton Transactions.

Supporting Information

to the paper entitled

Cryogenic magneto-caloric effect and magneto-structural correlations in carboxylate-bridged Gd(III) compounds

O. Roubeau, G. Lorusso, S. J. Teat and M. Evangelisti

Table of Contents

Table S1. Relevant magneto-structural parameters of Gd(III) compounds	p. S2
Figure S1. Labeled view of two successive Gd···Gd bridges along the coordination chains in the structure of **1**	p. S3
Figure S2. Labeled view of the two successive slightly different Gd···Gd bridges along the coordination chains in the structure of **2**.	p. S4
Figure S3. Field dependence of isothermal magnetization for **1** and **2** at 2 K	p. S5
Figure S4. Temperature dependence of χ^{-1} for **1** and **2**	p. S5
Figure S5. Temperature dependence of S_m for **1** and **2**	p. S6
Figure S6. Field dependence of isothermal magnetization for **1** and **2** at 2-10 K	p. S7
Figure S7. Magnetic entropy changes for **1** and **2** normalized to *R*	p. S8
Figure S8. Magneto-structural correlations for Gd(III) pairs with A- and B-type bridges.	p. S9
References	p. S10

Table S1. Magneto-structural parameters of Gd(III) compounds with only two μO:κ^2OO carboxylic bridges, so-called A-type bridge[#] and two μO:κ^2OO and two μOO *syn*-*syn* carboxylic bridges, so-called B-type bridge.

Compound[a]	Gd–O–Gd (°)	$d_{Gd\cdots Gd}$ (Å)	$d_{Gd–O}$ (Å)	Topology	*J* (cm^{-1})[b]	Ref.
A-type						
$[Gd_2(CH_3CO_2)_6(H_2O)_4]\cdot 4H_2O$	115.48	4.206	2.402/2.571	dinuclear	0.060	1
$[Gd_2(CH_3CO_2)_6(H_2O)_4]\cdot 4H_2O$	115.31	4.183	2.393/2.558	dinuclear	0.060	2
$[NH_3C_2H_5][Gd(Cl_2CHCO_2)_4]$[c]	113.50	4.181	2.443/2.556	1D alt.	0.058	3
$[Gd_2(mal)_3(H_2O)_6]_\infty$[d]	116.8	4.2763	2.308/2.597	3D/dinuclear	0.048	4
$[NH_3CH_3][Gd(Cl_2CHCO_2)_4]_\infty$[c]	114.07	4.184	2.449/2.538	1D alt.	0.046	5
$\{[Gd(cit)(H_2O)_2]\cdot H_2O\}_\infty$	118.49	4.321	2.508/2.521	1D/dinuclear	0.039	6
$[Gd_2(CH_3CO_2)_2(dbm)_4(MeOH)_2]$	113.65	4.128	-	dinuclear	0.038	7
$[Gd_2(CH_3CO_2)_6(H_2O)_4]\cdot 2H_2O$	115.47	4.1589	2.378/2.539	dinuclear	0.031	8
$[Gd(Hnica)(H_2O)_2(SO_4)]_\infty$[e]	113.35*	4.2555*	2.4505/2.6445*	1D alt.	0.030	9
$\{[Gd_2(ox)(fum)_2(H_2O)_4]\cdot 4H_2O\}_\infty$	119.1	4.5816	-	3D/1D	0.019	8
2 $\{[Gd(butOH)_3(H_2O)]\cdot H_2O\}_\infty$	113.375*	4.1115*	2.3925/2.5265*	3D/1D	0.0132	this work
$[Gd_2(tpac)_6(H_2O)_4]$	112.5	4.1255	2.412/2.547	dinuclear	–0.014	10
$[Gd_2(pac)_6(H_2O)_4]$	113.16	4.1215	2.394/2.543	dinuclear	–0.0309	10
B-type						
$[Gd_2(Hsal)_6(H_2O)_8]$[f]	-	4.25	-	dinuclear	0.050	11
$[Gd_2(Cl_2CHCO_2)_6(H_2O)_2(hypy)_2]$	107.64	4.051	2.378/2.638	dinuclear	–0.022	12
$[Gd(CF_2HCO_2)_3(phen)]$	106.92	4.034	2.354/2.662	dinuclear	–0.032	13
$[Gd_2(ClCH_2CO_2)_6(bipy)_2]$	106.585	3.99	2.372/2.602	dinuclear	–0.040	14
$[Gd_2(CH_3CO_2)_6(phen)_2]$	102.5	4.035	2.441/2.726	dinuclear	–0.053	15
$[Gd_2(CH_3CO_2)_2(fum)_2(H_2O)_4]_\infty$	105.9	3.866	-	2D/dinuclear	–0.076	8
$[Gd(Bz)_3(dmf)]_\infty$[g]	105.801	3.914	2.325/2.578	1D alt.	–0.097	16

[#] Compound $[Gd_4(CH_3CO_2)_4(acac)_8(H_2O)_4]$ is not included because its alternate chain structure involves successive A-type and di(μO:κ^2OO-carboxylato) bridges, while only one interaction constant has been derived.[7] Compound $\{Gd_4(bta)_3(H_2O)_{16}]\cdot 12H_2O\}_\infty$ is not included either, although its 3D structure is built on mononuclear and dinuclear Gd(III) units, the latter with A-type bridge.[17] The reported exchange coupling interaction was however apparently derived using a model considering only the dinuclear units, and is therefore probably not reliable. [a] abbreviations: H_2mal = malonic acid; cit = citrate ion, $(C_6H_5O_7)^{3-}$; Hdbm = dibenzoylmethane; H_2nica = 2-hydroxynicotinic acid; H_2ox = oxalic acid; H_2fum = fumaric acid; HbutOH = 4-hydroxybutanoic acid; Htpac = 3-thiophenacetic acid; Hpac = pentanoic acid; H_2sal = salicylic acid; hypy = 4-(1H)-pyridone; phen = phenantroline; bipy = 2,2'-bipyridine; HBz = benzoic acid; dmf = N,N'-dimethylformamide; Hacac = 2,4-pentandione or acetylacetone; H_4bta = 1,2,4,5-benzenetetracarboxylic acid. b Exchange constant are those corresponding the Hamiltonian $\boldsymbol{H} = -J\boldsymbol{s}_i\boldsymbol{s}_j$. [c] The 1D structure in these compounds is built on alternating A-type ferromagnetic and tetra(μO:κ^1O:κ^1O'-carboxylato) antiferromagnetic bridges, and an interaction constant has been derived for both. The former dominates the magnetic properties, and the data given here correspond only to the A-type bridge. [d] Structure made of dinuclear unit with A-type bridges connected into a 3D network through the malonate ligands. [e] the structure of this compound is made of 1D chains with very similar alternate A-type bridges, except one of these bridges has an additional sulfate bridge. [f] The structure of this compound is not known, but WAXS data confirm its similarity to the reported Er analogue and provide an evaluation of the Gd···Gd separation. [g] The 1D structure in this compound is built on alternating B-type and di(μO:κ^1O:κ^1O'-carboxylato) bridges, but the magnetic properties have been modeled with a dimer model with one sole interaction constant, ascribed to the B-type bridge. * Average values of the structurally different bridges, two very similar in **2** and two quite dissimilar in $[Gd(Hnica)(H_2O)_2(SO_4)]$. The value given for **2** derives from zJ/k_B = 0.052 cm^{-1} (see text) and z = 4, as an average value.

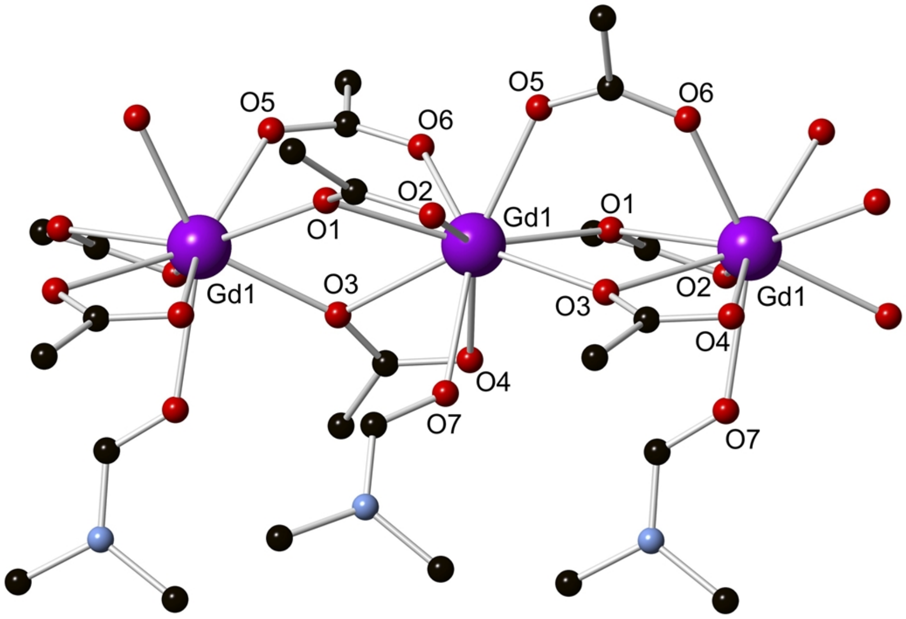

Figure S1. Labeled view of two successive Gd···Gd bridges along the coordination chains in the structure of **1**. The Gd1-O1-O3-Gd1 planes are tilted by 59.8º, but the chain remains close linear with a Gd···Gd···Gd angle of 174.15º.

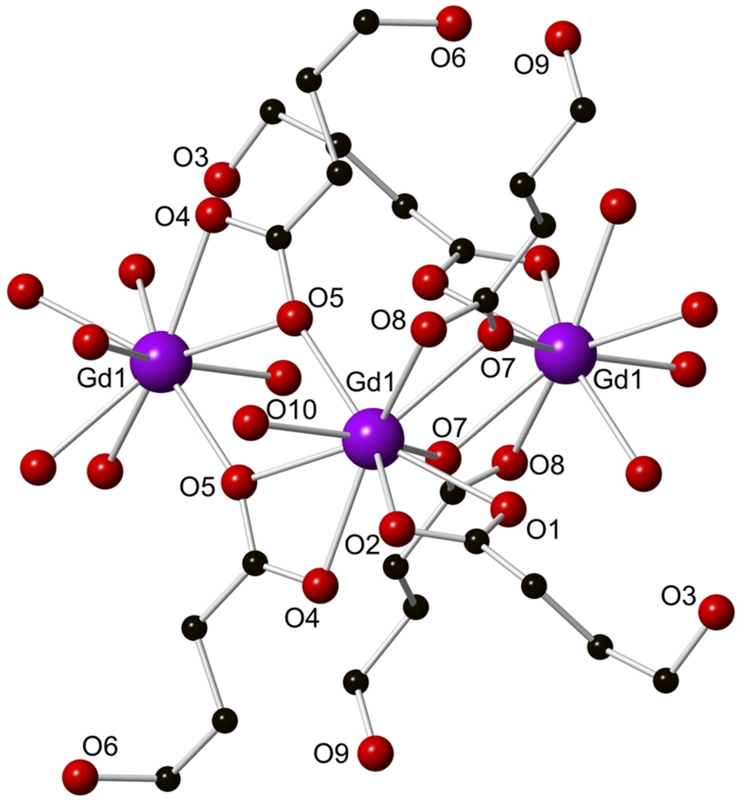

Figure S2. Labeled view of the two successive slightly different Gd···Gd bridges along the coordination chains in the structure of **2**. The Gd1-O5-O5-Gd1 and Gd1-O7-O7-Gd1 planes 87.4º, resulting in a zig-zag chain with a Gd···Gd···Gd angle of 98.23º.

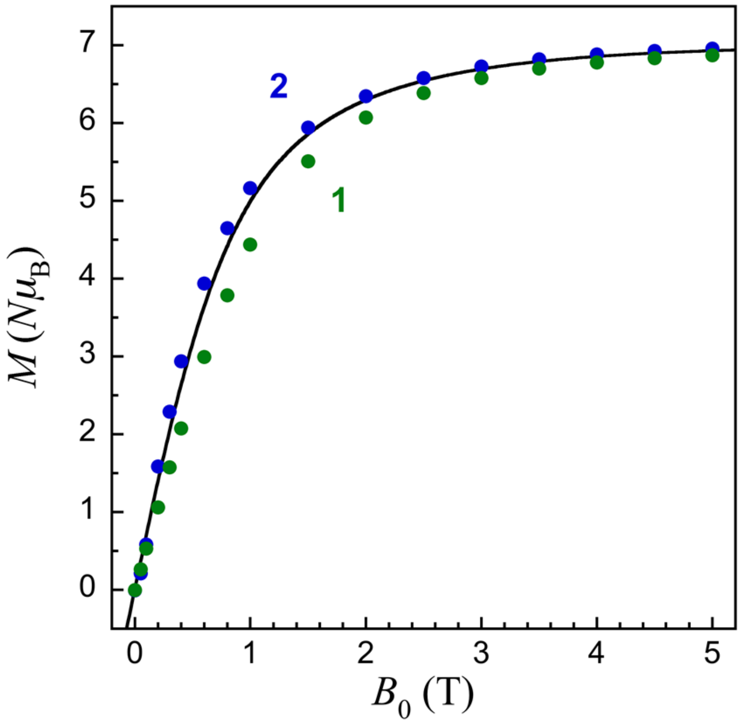

Figure S3. Field dependence of isothermal magnetization for **1** (green dots) and **2** (blue dots) at 2 K. The full line is the Brillouin function for *S* = 7/2 and *g* = 2.

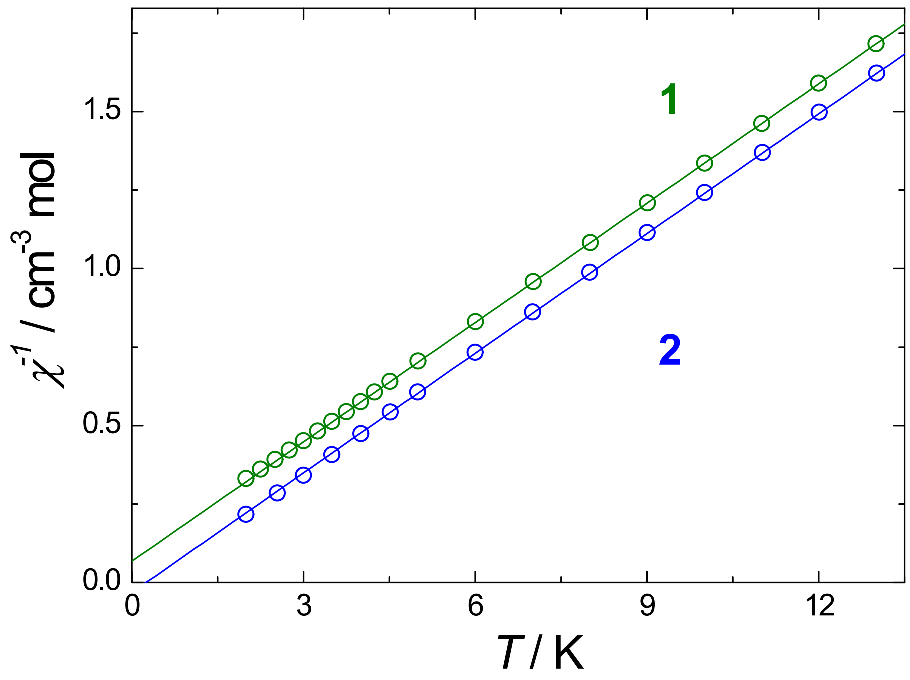

Figure S4. Inverse of magnetic susceptibility χ^{-1} vs *T* for **1** and **2**. Solid lines are best fits of Curie-Weiss law.

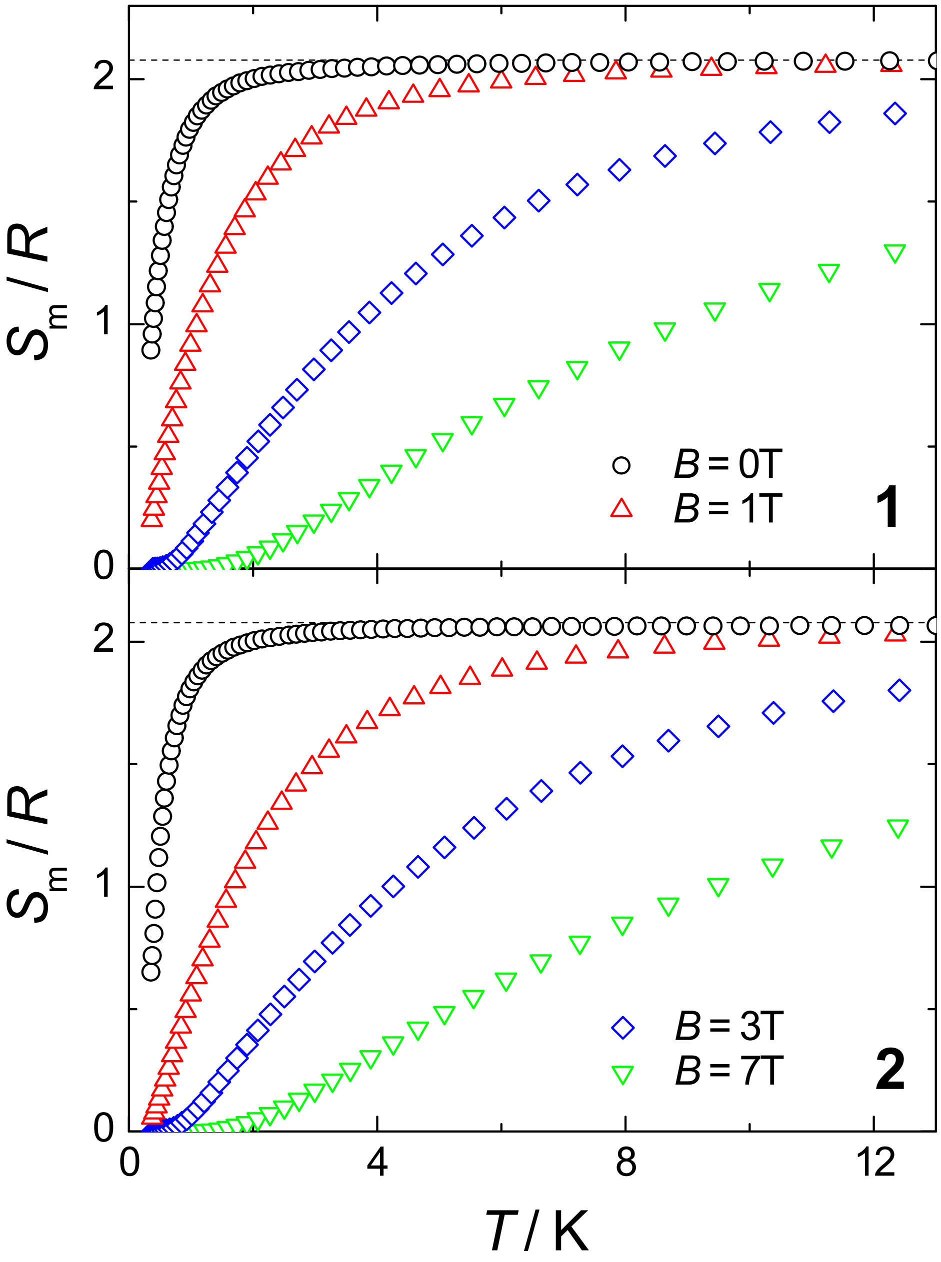

Figure S5. Temperature dependence of the experimental entropy normalized per Gd(**III**) ion and R, for **1** (top panel) and **2** (bottom panel). We cope with the lack of specific heat data at the lowest temperatures and B = 0 and 1 T (see Fig. 4) by scaling S_m / R to the high-temperature limit $\ln(s_{Gd}+1)$, as dashed lines.

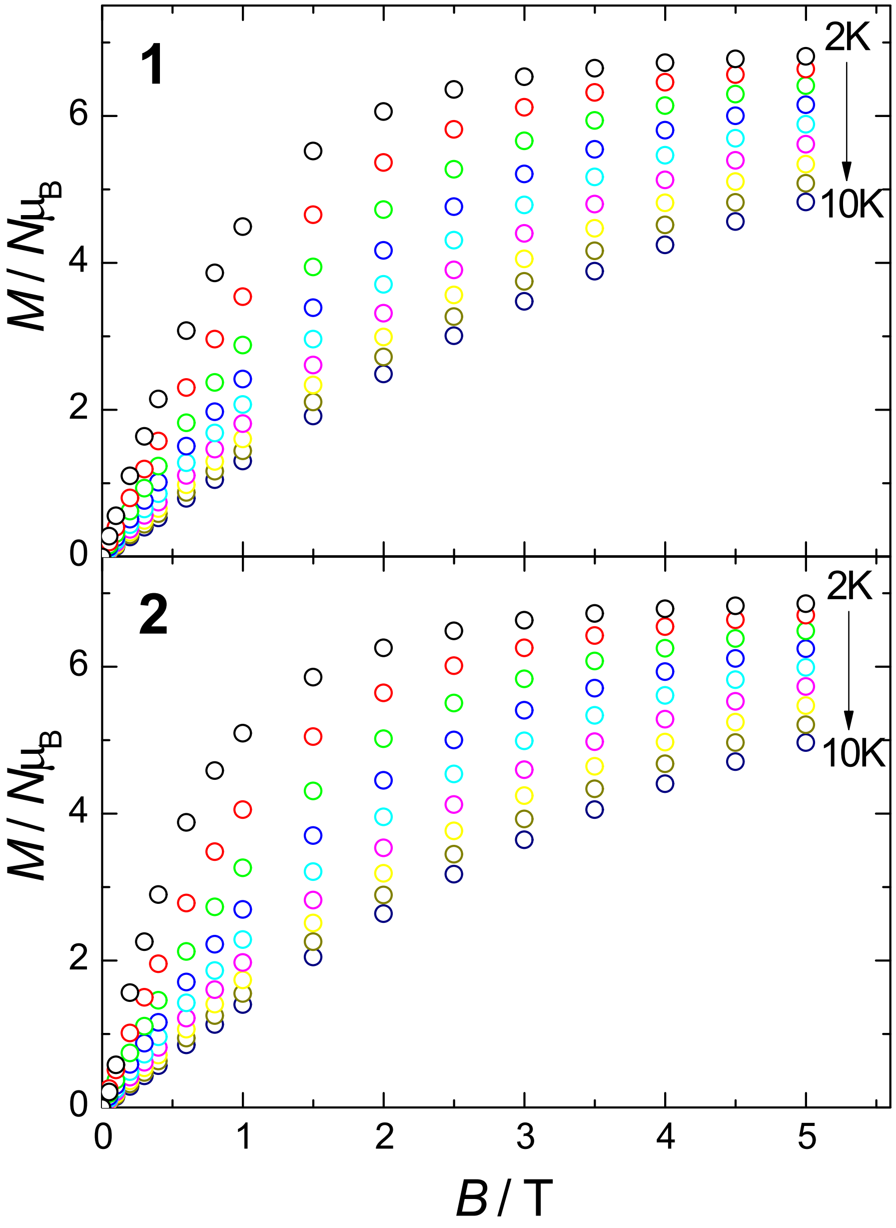

Figure S6. Field dependence of isothermal magnetization for **1** (top) and **2** (bottom) in the temperature range 2 – 10 K.

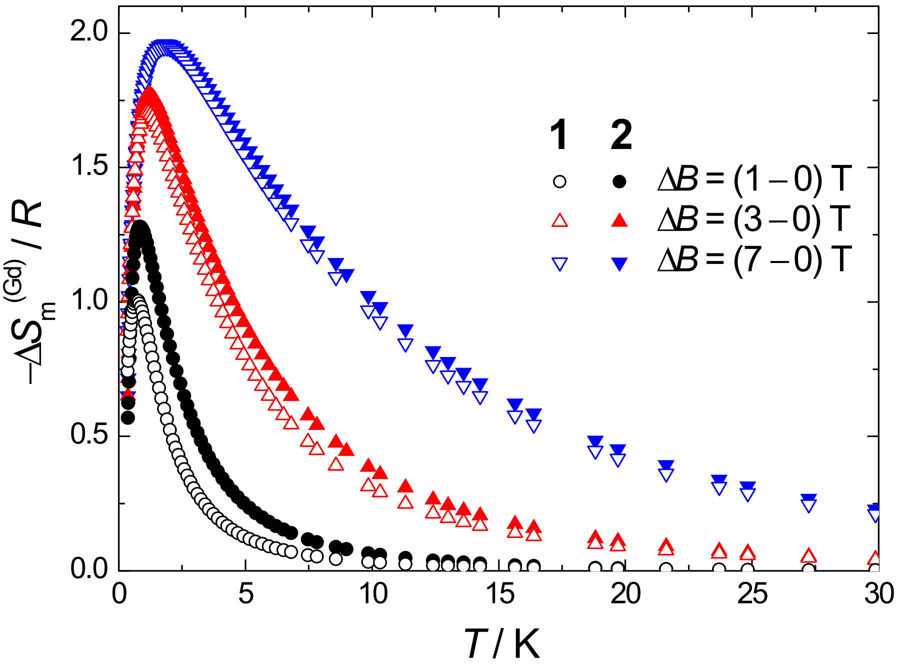

Figure S7. Temperature-dependencies of the magnetic entropy change, ΔS_m, normalized to Gd(III) ions and gas constant R, for the indicated applied-field changes ΔB, as obtained from specific heat data for **1** (filled markers) and **2** (empty markers).

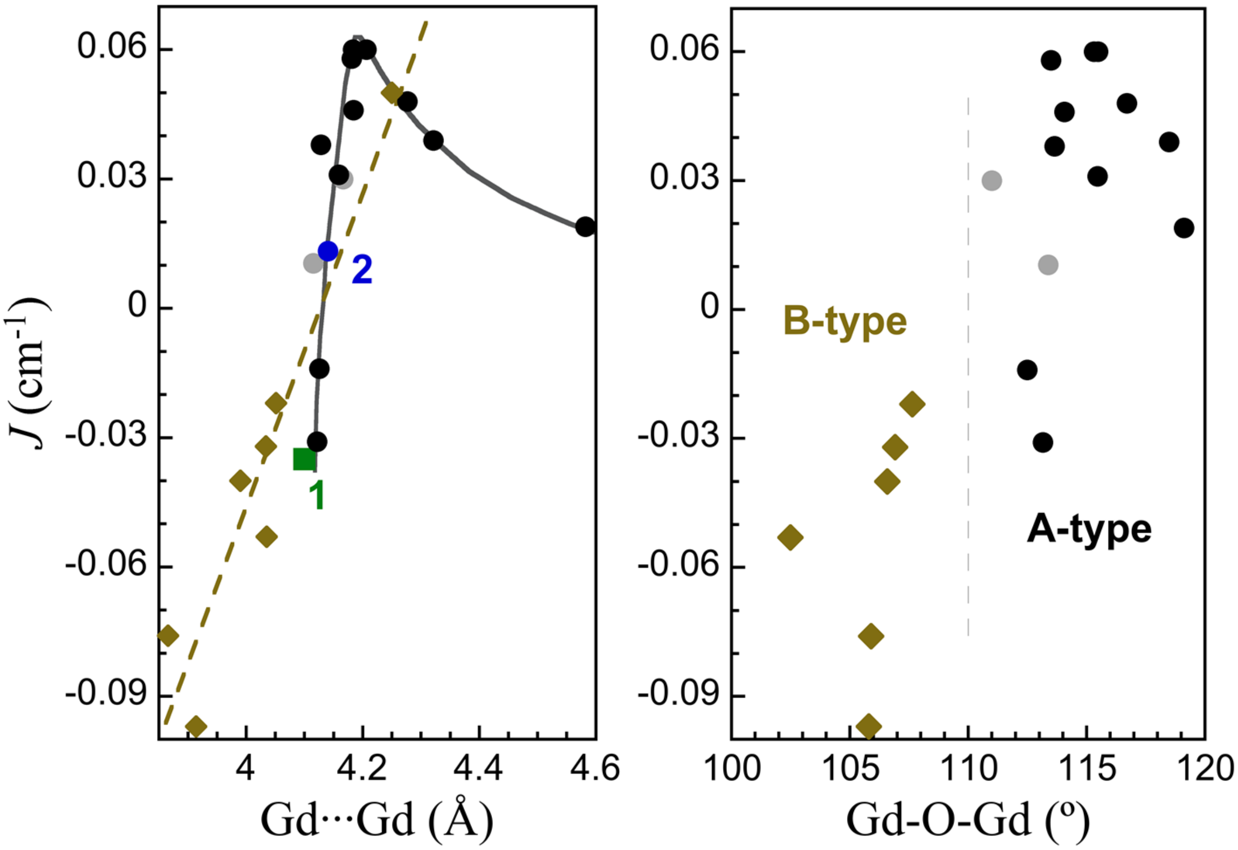

Figure S8. Correlation of the exchange coupling in Gd(III) pairs bridged by either two μO:κ^{2}OO carboxylates (A-type, black dots) or two μO:κ^{2}OO and two μOO *syn*-*syn* carboxylates (B-type, brown rhombs), respectively vs. the Gd···Gd separation (left) and the Gd–O–Gd angle (right). Grey dots are compounds with two different di(μO:κ^{2}OO carboxylate) bridges for which average values of the Gd···Gd separation and Gd–O–Gd angle have been used. The full line is a guide for the eye highlighting the reasonable correlation of data for A-type bridges. The brown dashed line is a linear fit of the data for B-type bridges. The value given for **2** derives from zJ/k_B = 0.052 cm^{-1} (see text) and z = 4, as an average value.

References.

1 a) S. T. Hatscher, W. Urland, *Angew. Chem. Int. Ed.* **2003**, 42, 2862-2864; b) M. C. Favas, D. L. Kepert, B. W. Skelton, A. H. White, J*. Chem. Soc. Dalton* **1980**, 454-458
2 M. Evangelisti, O. Roubeau, E. Palacios, A. Camón, T. N. Hooper, E. K. Brechin, J. J. Alonso, *Angew. Chem. Int. Ed.* **2011**, 50, 6606-6609
3 A. Rohde, W. Urland, *J. Alloys Compd.* **2006**, 408-412, 618-621
4 M. Hernández-Molina, C. Ruiz-Pérez, T. López, F. Lloret, M. Julve, *Inorg. Chem.* **2003**, 42, 5456-5458
5 A. Rohde, W. Urland, *Z. Anorg. Allg. Chem.* **2005**, 631, 417-420
6 R. Baggio, R. Calvo, M. T. Garland, O. Peña, M. Perec, A. Rizzi, *Inorg. Chem.* **2005**, 44, 8979-8987
7 F-S. Guo, J-D. Leng, J-L. Liu, Z-S. Meng, M-L. Tong, *Inorg. Chem.* **2012**, 51, 405-413
8 L. Cañadillas-Delgado, O. Fabelo, J. Cano, J. Pasán, F. S. Delgado, F. Lloret, M. Julve, C. Ruiz-Pérez, *CrystEngComm* **2009**, 11, 2131-2142
9 N. Xu, W. Shi, D-Z. Liao, S-P. Yan, P. Cheng, *Inorg. Chem.* **2008**, 47, 8748-8756
10 L. Cañadillas-Delgado, O. Fabelo, J. Pasán, F. S. Delgado, F. Lloret, M. Julve, C. Ruiz-Pérez, *Dalton Trans.* **2010**, 39, 7286-7293
11 J-P. Costes, J. M. Clemente-Juan, F. Dahan, F. Nicodème, M. Verelst, *Angew. Chem. Int. Ed.* **2002**, 41, 323-325
12 D. John, W. Urland, *Eur. J. Inorg. Chem.* **2006**, 3503-3509
13 D. John, W. Urland, *Z. Anorg. Allg. Chem.* **2005**, 631, 2635-2637
14 D. John, W. Urland, *Eur. J. Inorg. Chem.* **2005**, 4486-4489
15 A. Panagiotopoulos, T. F. Zafiropoulos, S. P. Perlepes, E. Bakalbassis, I. Masson-Ramade, O. Kahn, A. Terzis, C. P. Raptopoulou, *Inorg. Chem.* **1995**, 34, 4918-4920
16 A. W-H. Lam, W-T. Wong, S. Gao, G. Wen, X-X. Zhang, *Eur. J. Inorg. Chem.* **2003**, 149-163
17 L. Cañadillas-Delgado, J. Pasán, O. Fabelo, M. Julve, F. Lloret, C. Ruiz-Perez, *Polyhedron* **2013**, 52, 321-332